Effect of processing temperature on the texture and shear mechanical properties of diffusion bonded Ti-6Al-4V multilayer laminates

C.M. Cepeda-Jimenez[1], A. Orozco-Caballero[1], A. A. Sarkeeva[2], A.A. Kruglov[2], R.Ya. Lutfullin[2], O.A. Ruano[1], F. Carreño[1]

[1]Department of Physical Metallurgy, CENIM, CSIC, Av. Gregorio del Amo 8, 28040 Madrid, Spain

[2]Institute for Metals Superplasticity Problems, 39 Khalturina St., Ufa 450001, Russia

Abstract

Two multilayer materials based on Ti-6Al-4V alloy have been processed by diffusion bonding at two different temperatures (1023 K (750 ºC) and 1173 K (900 ºC)). The influence of the processing temperature on microstructure, texture and mechanical properties of the two multilayer materials has been analyzed. Scanning electron microscopy, X-ray diffraction, electron backscatter diffraction (EBSD), and shear tests have been used as experimental techniques. The multilayer laminate processed at the lowest temperature of 1023 K (750ºC) presents mainly transversal texture in the longitudinal plane, which provides an anisotropic mechanical behavior, showing higher shear modulus and maximum shear strength under one of the shear test directions considered. In contrast, diffusion bonding at 1173 K (900 ºC) leads to basal/transversal texture due to the partial $\alpha \rightarrow \beta \rightarrow \alpha$ transformation, which provides more isotropic mechanical properties. Accordingly, this laminate shows similar shear modulus and maximum shear strength in different shear test orientations.

Keywords: A. Microstructure; A. Texture; B. Ti-6Al-4V multilayer laminate; C. Diffusion bonding; D. Mechanical properties

*Corresponding author. Tel.: +34 91 5538900; fax: +34 91 5347425.

E-mail address: cm.cepeda@cenim.csic.es (C.M. Cepeda-Jiménez)

1. Introduction

The two-phase α-β Ti–6Al–4V alloy is well known for aerospace applications because of its low density, high strength, excellent corrosion resistance, and good high temperature durability [1,2].

Multilayer composite materials can be developed in bulk form with strength and toughness properties far superior to those of their individual constituents [3]. Accordingly, multilayer materials made of titanium alloys can be considered as advanced materials for manufacturing various structural components [4].

Diffusion bonding is an attractive processing method to obtain multilayer materials [4]. This process is dependent on various parameters, in particular, time, applied pressure, and bonding temperature to promote microscopic atomic movement to ensure complete metallurgical bond [1]. The interfacial properties have been shown to greatly affect the mechanical behavior of composite laminates [5-7], because interfaces are numerous and susceptible to decohesion and sliding [8]. In a previous work [9], two multilayer materials based on high strength Ti–6 Al–4 V alloy were successfully processed by diffusion bonding considering two processing temperatures (1023 K (750 ºC) and 1173 K (900 ºC)), which determined the presence or not of pores at the interface. In this work, it was reported that processing at the highest temperature of 1173 K (900 ºC) led to high bonding degree, without noticeable Charpy impact toughness increase of the overall multilayer laminate. In contrast, processing at lower processing temperature of 1023 K (750 ºC) made difficult the healing of interfacial pores and voids, decreasing the interfacial toughness, which was determined by shear tests, and leading to an impact toughness value of the overall multilayer material seven times higher than the reported value for the as-received Ti–6 Al–4 V alloy. Thus, the presence of pores and defects induced during processing affects the mechanical strength of interfaces favoring delamination and crack renucleation as principal toughening mechanisms in multilayer materials, improving the material toughness [7,9].

On the other hand, unlike aluminum and steel alloys, titanium alloys may have a pronounced anisotropy of properties, which can be directly related to the inherent anisotropy of the hexagonal crystal structure of the α phase [10,11]. Additionally, titanium is characterized by two allotropic modifications: the β body centered cubic phase, stable at high temperature, and the α hexagonal close packed phase stable at room temperature. The phase transformation occurs at 882°C in pure Ti but it varies with the alloying elements. Both phases are well known to be related by the Burgers orientation relations $\{110\}\beta//\{00.2\}\alpha$ and $<111>\beta//<1\text{-}2.0>\alpha$ [12].

Concerning the phase transformation, a texture memory effect is often reported when the hexagonal α metal is heated, transforms into the cubic β phase and returns to the hexagonal α phase after cooling [13-16]. It is obvious that crystallographic textures may offer an opportunity to properly design the properties of titanium alloys in order to control the usually strong textures that are developed during different processing conditions.

Since the final texture of titanium alloys after processing influences the material properties at room temperature, it seems interesting to study the texture evolution of the Ti-6Al-4V multilayer materials previously processed by diffusion bonding at two different temperatures. As mentioned, one Ti-6Al-4V multilayer material has been processed at 1023 K (750 ºC), which corresponds to processing in the mainly α-phase

field, while the other one was processed at 1173 K (900 ºC) in the α/β phase field. Therefore, in this study, the main microstructural changes that seem to control the phase transformation and thus the final textures upon heating and cooling from the different processing temperatures are discussed. The texture of the diffusion bonded multilayer laminates has been analyzed by X-ray diffraction and the electron backscatter diffraction technique (EBSD). Finally, the relationship between final texture and the shear mechanical properties at room temperature and operative deformation mechanisms will be analyzed.

2. Experimental procedure

2.1. Materials and processing

Thirteen Ti-6Al-4V sheets of ~0.86 ± 0.02 mm in thickness were stacked, making up a bundle of ~10.9 mm in thickness, ~105 mm in width and ~220 mm in length. The as-received sheets were provided by VSMPO, Verhnyaya Salda, Russia. The composition (in weight per cent) of the Ti-6Al-4V alloy was 6.27 Al, 4.22 V, 0.18 Fe, less than 0.001 H, less than 0.01 N, 0.2 O and the balance titanium.

The multilayers materials were manufactured by diffusion bonding in a vacuum furnace under argon pressure. Processing was performed using two different regimes: 1) 1023 K (750 ºC) during 2 h and 3 MPa; and 2) 1173 K (900 ºC) during 2 h and 3 MPa. After processing, the multilayer materials were cooled in the vacuum furnace to room temperature, and additional thermal treatment was not performed.

The average thickness of the titanium layers in the laminates processed at 1023 and 1173 K (750 and 900 ºC) was ~860±8 μm and ~870±17 μm, respectively.

2.2. Microstructural determination

The microstructure of the as-received Ti-6Al-4V alloy and of the diffusion bonded laminates was analyzed by scanning electron microscopy (SEM) using a JEOL JXA-6400 equipment. The linear intercept method was used to estimate the grain size. At least 300 grains were analyzed to determine the grain size.

Macrotexture measurements were performed by X-ray diffraction (XRD) using CuK_α radiation in a Siemens D500 diffractometer equipped with an open Euler ring, working with Schultz geometry. From these measurements, (0001) and (10-10) pole figures were obtained.

In addition, electron backscatter diffraction (EBSD) was also employed in the present investigation, as a complementary technique to XRD. Although EBSD only allows examination of the local texture or microtexture, using EBSD software, it was possible to re-orientate the inverse pole figures to highlight the texture according to the various relevant directions of the shear tests. EBSD orientation maps were performed in

a scanning electron microscope (SEM) JEOL JSM6300, with a fully automatic EBSD attachment of Oxford Instruments, operating at an accelerating voltage and a working distance of 20 kV and 15 mm, respectively. The indexation of the Kikuchi lines and the determination of the orientations were done with the software INCA developed by Oxford Instruments. The area mapped for the multilayer laminates samples was 62 × 46 μm^2 with a step size of 0.24 μm. The microstructure is represented by EBSD orientation maps and the microtexture is represented by inverse pole figures recalculated from the EBSD orientation data. Sample preparation for EBSD included grinding with 2400 SiC paper, mechanical polishing with 9 and 1 μm diamond paste and a 0.05 μm silica suspension, and final electropolishing in a 10% perchloric acid solution in methanol at 248 K (-25 ºC) and 20 V during 10-15s.

In this work, to avoid confusion, a different notation for the sample reference system is used instead of the traditional RD, TD and ND directions. It is defined as follows: the interface direction is ID, the direction normal to the laminate is ND, and the transversal directions to the laminate plane are TD (Fig. 1a).

2.3. Mechanical properties. Shear test.

Shear tests have been performed to characterize the mechanical properties of the processed multilayer materials (Fig. 1b). A *Servosis* universal test machine (cross-head rate=0.005 mm/s) has been employed, using samples of approximate dimensions $10\times10\times3$ mm^3. For comparison, the Ti-6Al-4V multilayer laminates were tested in two different orientations, defined as interfacial and monolithic type configurations, and schematized in Fig. 1c. The tests were performed by clamping the samples between two metal supports (Fig. 1b). For testing in interfacial orientation, the interface to be tested is located just outside the border of the tool and parallel to the load direction (Fig. 1b and 1c). Then, a square punch at a given gap distance (l_{gap}) is used to apply the shear load until failure of the interface. For testing in a monolithic configuration (Fig. 1c), the multilayer materials were rotated 90 degrees, thus having the interfaces a negligible effect. Therefore, differences in mechanical behavior between different orientations can be evaluated.

The shear stress, τ, and the shear strain, γ, are given by the expressions [17]:

$$\tau = p/ae \qquad \gamma = \tan(\alpha) = d/l_{gap} \qquad (2)$$

where a is the initial width of the sample, e is the initial thickness, p is the force applied on the sample, d is the midspan displacement, α is the shear angle and l_{gap} is the distance between the supports and the mobile punch, corresponding to 0.35 mm in this study.

3. Results

3.1. Microstructure

The microstructure of the as-received Ti–6Al–4V alloy in the rolling plane is presented in Fig.2a, which consists of equiaxed α grains ~3 μm in size surrounded by the equilibrium volume fraction of β phase along grain boundaries of α grains. This equilibrium volume fraction of the β phase is typically less than 8 vol.% at room temperature [14].

Fig.2b and 2c show SEM micrographs corresponding to cross-sections, containing ID and ND directions as defined previously, of the two multilayer laminates processed at 1173 and 1023 K (900 and 750 ºC), respectively. The micrographs were taken including interfaces and these are located in the middle of the images. These micrographs suggest a very good bond, although further assessment of bond integrity requires quantitative mechanical testing.

After diffusion bonding, the microstructure of the Ti-6Al-4V alloy in the multilayer materials is characterized by equiaxed α grains, being 5.4 ± 1.8 and 2.9 ± 1.2 μm for the laminates processed at 1173 and 1023 K (900 and 750 ºC), respectively. At 1173 K (900 ºC), the Ti-6Al-4V alloy shows a slight α grain growth (~5.4 μm) in comparison with the as-received alloy (~3 μm) (Fig.2a). The volume fraction of the β phase at room temperature for both materials is considered to be similar, and equal to the mentioned value of about 8 vol.% for the as-received alloy [14].

As previously published [9], the interface between the two layers illustrates the presence of pores or voids. The relative length of pores (L_p) was ~32% for the laminate processed at low temperature (Fig.2c), while L_p in the interfaces is nearly negligible at higher processing temperature of 1173 K (900 ºC) (L_p~1%) (Fig. 2b).

Fig. 2d shows a schematic phase diagram for the Ti-6Al-4V alloy in the α+β region of interest for processing of multilayer materials in the present work. It is has been reported [18,19] that between 1023 and 1173 K (750 and 900 ºC) the proportion of β phase varies from about 10% to 50%. The proportion of α/β phases in the microstructure during diffusion bonding process will determine the texture of multilayer materials, and therefore the mechanical properties of the laminates, as will be discussed below.

To understand the mechanical properties of the two processed laminates as a function of the load direction, it is necessary to evaluate the nature of the texture after the two processing conditions considered. The texture was analyzed at the cross-section, in the longitudinal-transversal plane (LT), containing ID and ND directions, as shown in the laminate scheme depicted in Fig. 1a.

The pole figures for the basal plane (0001) and prismatic (10-10) planes of the α phase corresponding to the two multilayer laminates obtained by XRD are presented in Fig. 3a and b. In addition, the hexagonal unit cell of α phase is shown in Fig. 3c.

Various slip planes and slip directions for α titanium are indicated in the hexagonal unit cell. The main slip directions are the three close-packed directions of the type <11$\bar{2}$0>. The slip planes containing these slip directions are the (0001) plane, the three {10$\bar{1}$0} planes, and the six {10$\bar{1}$1} planes [20].

The Ti-6Al-4V multilayer laminate processed at 1173 K (900 ºC) (Fig. 3a) exhibited a strong basal/transverse texture (B/T) ({0001}<11$\bar{2}$0>/{10$\bar{1}$0}<11$\bar{2}$0>) (×9 random) in the analyzed LT plane. The term "basal texture" refers to texture with basal planes oriented parallel to the analyzed cross-section (LT plane). Likewise, "transverse texture" is referred to prismatic planes being parallel to the analyzed LT plane. It can be observed that the basal component is more intense than the transversal component, which presents the *c*-axis of the hcp α crystallites oriented along both the interface and the normal direction (see scheme in the inset of Fig. 3a corresponding to the LT plane).

The Ti-6Al-4V laminate processed at 1023 K (750 ºC) presents a weaker texture (×6 random), being mainly basal with little proportion of transversal texture components oriented mainly in the interface direction (ID), as observed in the pole figures and the corresponding scheme in Fig. 3b for the LT plane. It can be concluded, therefore, that the processing temperature influences the texture type of the processed multilayer laminates. Moreover, it is expected that the B/T texture observed for the laminate processed at higher temperature (1173 K (900 ºC)) provides more isotropic mechanical properties, than those of the laminate processed at 1023 K (750 ºC) with a predominately basal texture. This will be discussed extensively below.

3.2. Mechanical properties. Shear tests.

Shear tests have been performed to characterize precisely the mechanical properties of the multilayer materials. Figure 4a shows a plot of shear stress versus shear strain obtained from shear tests on both test orientations considered (Fig. 1c).

In addition, Fig.4b shows shear curves obtained for the multilayer laminates processed at 1173 and 1023 K (900 and 750 ºC) tested in interfacial test orientation. Several samples for every configuration were tested and different tested interfaces are labeled by numbers indicating their location in the multilayer material with respect to the outer layer (e.g. s3-i5 means sample 3 and the fifth interface from the surface). It can be observed that the results are very reproducible, as demonstrated by the perfect overlapping of all curves corresponding to each material configuration selected. Table 1 includes average values of mechanical properties calculated from various shear curves of different material configurations.

Clear differences in shear modulus (slope of the curve in the elastic region, which is normally referred as structural stiffness) and maximum shear strength (τ_{max}) are observed between different curves depicted in Fig. 4a. It can be observed that the

laminate processed at 1023 K (750 ºC) presents higher shear modulus and τ_{max} when is tested in the monolithic configuration. However, the laminate processed at higher temperature (1173 K (900 ºC)) presents similar shear modulus and τ_{max} values in both tested orientations (monolithic and interfacial) (Fig. 4a), and also close to those for the laminate processed at 1023 K (750 ºC), oriented for testing its interfaces. In fact, the Ti-6Al-4V alloy in monolithic configuration shows average values of maximum shear stress between 481 and 547 MPa, and shear strain between 2.61 and 2.07 for the laminates processed at 1173 and 1023 K (900 and 750 ºC), respectively (Fig.4 and Table 1). In general, all interfaces of the multilayer materials present lower strength and ductility than those of the monolithic alloy configurations.

Regarding the Ti-6Al-4V multilayer laminate processed at high temperature, fracture in the interfacial test orientation occurred at the point of maximum stress (~502 MPa) with nearly instantaneous debonding at interface, as indicated by an abrupt unloading on the stress-strain curves shown in Fig. 4a and b, showing values of shear deformation to failure ranged between 1.25 and 1.41. In contrast, the multilayer material tested at 1023 K (750 ºC), which showed high degree of porosity in interfaces [9], shows interfaces quite brittle, with lower values of maximum shear stress (455 MPa) than the laminate processed at 1173 K (900 ºC), and also lower values of shear deformation to failure ranged between 0.77 and 0.90 (Fig. 4a and b).

However, the large differences in shear modulus and τ_{max} of the monolithic 750ºC sample, which are attributed to the inherent anisotropy of α phase of titanium and the texture developed during diffusion bonding processing, remains to be explained and will be analyzed below.

4. Discussion

In the present work, two multilayer materials based on the Ti-6Al-4V alloy have been processed by diffusion bonding at two different temperatures, 1023 and 1173 K (750 and 900 ºC). According to the obtained results, the processing temperature influences the type of texture, and thus, the mechanical properties of multilayer materials, which have been determined by shear tests.

4.1. Microstructure and texture of the processed multilayer materials

The microstructure of both processed multilayer materials is characterized by equiaxed α grains (Fig. 2). It is has been reported [20] that a fully equiaxed structure with the equilibrium volume fraction of β phase located at the "triple-points" of α grains is obtained if the cooling rate from recrystallization annealing temperature is sufficiently low. In the current work, the samples were slowly cooled inside the vacuum

furnace from the processing temperature to room temperature, which justifies the equiaxed grains obtained.

A comparison of the microstructure of the multilayer material processed at 1023 K (750 ºC) (Fig. 2c) respect to that processed at 1173 K (900 ºC) (Fig.2b) reveals that the grain size of the laminate processed at low temperature, i.e. where α phase is predominant (Fig. 2d), is maintained stable, having a fine grain size (~2.9 μm). At the higher processing temperature of 1173 K (900 ºC) (~1%), some grain growth (~5.4 μm) in comparison with the as-received alloy (~3 μm) (Fig. 2a) was observed. The increase in processing temperature up to 1173 K (900 ºC) emerges the presence of high-temperature β phase, where the β volume fraction is about 50% at 1173 K (900 ºC) (Fig. 2d), much higher than the 10% for the laminate processed at 1023 K (750 ºC) [18,19]. The presence of this β phase and the high temperature of 1173 K (900 ºC) accelerates grain growth, as evidenced in Fig. 2b after the partial β→α transformation after cooling to room temperature [21]. It has been reported [15] that in the two-phase α/β region, the high-temperature β phase is mainly obtained by the growth of β nuclei that exist at room temperature. In addition, if a primary α phase is present at high temperature, grain growth of this phase is also favored by diffusion of vanadium solutes through the β matrix. It is to note that, although grain size influences the mechanical behavior of Ti alloys, the small difference in grain sizes observed between the two multilayer materials investigated is not important for this study.

However, as mentioned, at low processing temperature of 1023 K (750 ºC), the proportion of β phase is low and the harder α phase dominates the deformation behavior. Generally, the number of independent slip systems is only 4 for the polycrystalline hcp α titanium structure while it is at least 12 for the bcc lattice, justifying the limited plastic deformability of the hcp α titanium compared to the bcc β titanium. In addition, the diffusion coefficient of α titanium is orders of magnitude smaller than that of bcc β titanium because of the densely packed atoms of the hcp structure [22]. This limited plastic deformability and diffusion of the hcp α phase explained the high volume fraction of pores in interfaces for the multilayer laminate processed at 1023 K (750 ºC), and the difficulty for healing them during processing (Fig. 2c) [9].

In contrast, at highest processing temperature of 1173 K (900 ºC), the properties of the Ti-6Al-4V alloy are controlled by the softer β phase. In general, this phase facilitates rotation, translation and rearrangement of α grains, being the properties of the β phase more apparent [23] and thus, justifying the high bonding degree observed (Fig.4a and b).

On the other hand, it is well known that the two phase (α + β) titanium alloys upon plastic deformation exhibit texture generation and significant mechanical property anisotropy due to the hexagonal close packed α phase [24]. In our case, since the plastic deformation is very small during the diffusion bonding processing, the different crystallographic textures of the multilayer laminates must have been inherited from the as-received material, and are only modified by the processing temperatures.

As determined by XRD, the Ti-6Al-4V multilayer laminate processed at 1023 K (750 ºC) showed a weak texture in the LT plane (Fig. 3b), presenting mostly basal texture with little proportion of transversal texture components oriented mainly in the interface direction (ID). In contrast the laminate processed at 1173 K (900 ºC) (Fig. 3a) exhibited a strong basal/transverse texture ($\{0001\}\langle 11\bar{2}0\rangle$ /$\{10\bar{1}0\}\langle 11\bar{2}0\rangle$) in the LT plane, being the basal component slightly more intense than the transversal components (see scheme in the inset of Fig. 3a). According to these results, and taking into account that the same as-received material was considered to process both multilayer materials, it can be asserted that the processing temperature influences the final texture.

Taking into account the orthorhombic symmetry of the as-received rolled sheets, Fig. 3 includes the main texture components corresponding to the longitudinal (L) plane, having been estimated from the textures analyzed by XRD in LT sections. Accordingly, it can be observed that the texture in the L plane for the laminate processed at 1023 K (750 ºC) is mainly transversal (T), while it continues being basal/transversal (B/T) for the laminate processed at 1173 K (900 ºC).

It has been reported [25] that high temperature deformation in the (α+β) phase field or close to the β transus results in a T texture, while deformation at lower temperature (for example below about 850°C for the Ti-6Al-4V alloy) leads to a B/T texture. In addition, the intensity of the T texture is usually low as compared to the B/T texture because of the higher deformation temperature. Therefore, the low intensity of texture in the processed material at 1023 K (750 ºC) in the longitudinal plane (L), as observed in the scheme included in Fig. 3b, having mainly a T component along TD, allows us to deduce that the texture of this laminate is inherited from the as-received material, which was rolled at high temperature. Furthermore, it has been reported [21] that texture remains constant during annealing at temperatures below the phase transformation. Therefore, in our study, the diffusion bonding temperature of 1023 K (750 ºC) can be considered a temperature that does not modify the as-received rolling texture.

On the contrary, a partial α→β transformation occurs during diffusion bonding processing at 1173 K (900 ºC), and later another partial β→α transformation occurs during cooling to room temperature in the vacuum furnace. Accordingly, after slow cooling back to room temperature, the material is largely hexagonal again, and the texture is slightly stronger (×9 random), as observed in Fig. 3a, with the (0001)

maximum splitted into two submaxima (B/T texture). Thus, the main difference with respect to the processed material at 1023 K (750 ºC), with mainly basal texture in the LT plane, is that the new *hcp* texture presents maxima in the basal and transversal components (Fig. 3a). In general, in Ti–6Al–4V alloy, a texture memory effect has been observed after the successive partial $\alpha \rightarrow \beta \rightarrow \alpha$ transformation [15]. In addition, the final α texture was quite sharp and new orientations are observed, as in the current work. Thus, after cooling ($\beta \rightarrow \alpha$ phase transformation) the α phase present at high temperature maintains its orientations relatively similar to those observed before heating, although a pronounced increase in density around the main texture components is favored during grain growth [15]. Furthermore, it has been reported that the high temperature β phase is mainly obtained by the growth of pre-existing β nuclei [14,26]. This consequently tends to favor specific β grain orientations with minimal misorientations, and justify the new orientations after the $\beta \rightarrow \alpha$ transformation according to the Burgers relationship. Therefore, the successive partial $\alpha \rightarrow \beta \rightarrow \alpha$ transformation taking place for the laminate processed at 1173 K (900 ºC) leads to the strong B/T texture observed.

Figure 5 shows EBSD maps for the different sections of the Ti-6Al-4V multilayer laminate processed at 1023 K (750 ºC), according to the laminate scheme included in Fig. 1a. The EBSD software allows re-calculating the orientation maps to depict the microtexture as seen from a different orientation. The interface is located approximately in the middle of the maps, and the non-indexed points correspond to pores distributed continuously along the interface. In addition, inverse pole figures corresponding to regions located to both sides of the interface in Fig. 5a have been also included. From these IPFs, it can be concluded that, although the analyzed area is limited, the microtexture is nearly the same at both sides from the interface. As will be seen below, textures calculated from the EBSD maps will serve us to prove the goodness of the macrotexture estimation (main components) made by XRD for the different sections of the laminates (Fig. 3).

4.2. Mechanical properties and relationship with the texture of the processed multilayer materials.

From shear tests it was observed that, in general, all interfaces of the multilayer materials present lower strength and ductility than those of the monolithic alloy configurations (Fig. 4a). In a previous work [9] the Charpy impact toughness for the multilayer processed at 750 ºC was measured, being seven times higher than that for the as-received Ti–6 Al–4 V alloy. This outstanding toughness increase was due to the high volume fraction of pores in its interfaces, which favors delamination across the interfaces and subsequent crack renucleation, warranting large absorbed energy.

In contrast, at the high processing temperature of 1173 K (900 ºC) high bonding degree was observed, with an interface nearly imperceptible (Fig.2b), due to the high diffusivity at this temperature and, as previously reported [27], shift and/or rotation of grains relative to each other in the vicinity of bonded interfaces due to grain boundary sliding (GBS).

In addition, from the shear curves depicted in Fig. 4a, it can be concluded that the mechanical properties are rather isotropic for the laminate processed at 1173 K (900 ºC), showing similar shear modulus (stiffness) and maximum shear strength (τ_{max}) tested in different orientations (interfacial and monolithic). This isotropy in the mechanical properties can be considered as an advantage, taking into account the intrinsic anisotropic character of the hexagonal crystal structure of the α phase. In contrast, the multilayer laminate processed at 1023 K (750 ºC) showed higher shear modulus (stiffness) and maximum shear strength (τ_{max}) in the monolithic test configuration than in the interfacial test configuration (Fig. 4.a and Table 1). This different mechanical behavior is related to the nature and intensity of the texture, as will be analyzed below.

Fig. 6 illustrates different schemes corresponding to the relative orientation between the laminate planes and the shear load direction (SLD) for all tests performed (interfacial and monolithic configuration). In these schemes, the laminate reference system (ID, TD, ND) employed in this work is also included and the corresponding rotations performed around the reference axis to test the laminates in different configurations. Accordingly, Fig. 6a and Fig. 6b correspond to the orientations considered for the laminate processed at 1023 and 1173 K (750 and 900ºC), respectively. Furthermore, for an easier visualization of the influence of texture on the mechanical properties with respect to the shear load direction (SLD), the main positions of the hexagonal unit cell for the different sections is sketched for both laminates. These main texture components in each laminate section have been estimated from the macrotextures obtained by XRD in the LT plane (Fig. 3), taking into account that the current system is orthogonal. Moreover, as mentioned previously, thanks to the use of EBSD, which allows re-orientation of the inverse pole figures as seen from the loading direction, the corresponding IPFs have also been included to corroborate the estimated textures from XRD. In all cases, the main texture components estimated from XRD results are backed by the IPFs from EBSD.

It is well known that the main dislocation slip mode in titanium at room temperature is the prismatic $\{10\bar{1}0\}<11\bar{2}0>$ slip system, which is followed in importance by the basal $\{0001\}<11\bar{2}0>$ slip system (Fig. 3b) [28], being the main slip directions ($<11\bar{2}0>$) parallel to the basal plane. Additionally, dislocation glide on pyramidal systems $<11\bar{2}0>\{10\bar{1}1\}$ and $<11\bar{2}3>\{10\bar{1}1\}$ can also be activated [29].

Clearly, therefore, the orientation of the prismatic planes will play a key role in the deformation response of the alloy and hence its shear mechanical properties [28].

Fig. 6a-3, corresponding to the laminate processed at 1023 K (750 ºC) and tested in monolithic orientation, shows that basal planes were mostly perpendicular to the shear axis and thus prismatic planes were predominantly parallel to it. In such instances, where the *c*-axis is near parallel to the loading direction, slip on the prismatic plane is not favored because the dislocation Burgers vector is parallel to the basal plane (<11$\bar{2}$0>) and the shear stress is zero in this case [30]. Although the few remaining basal planes parallel to the shear direction can be active, the limited number of prismatic slip systems available could be related to the higher shear modulus and τ_{max} observed for this configuration (Fig.4a and Table 1).

In contrast, the multilayer laminate processed at 1173 K (900 ºC) (Fig. 6b), which showed a stronger B/T texture after diffusion bonding (Fig. 4a), presents grains favorably orientated for prismatic slip ({10$\bar{1}$0}<11$\bar{2}$0>) in the two testing configurations (interfaces-Fig. 6b2 and monolithic-Fig. 6b3). These grains can be deformed at lower stresses, leading to larger plastic strains, as observed in Fig. 4a, and justify the lower shear modulus and τ_{max} observed for the laminate processed at 1173 K (900 ºC) in the two configurations tested with respect to the laminate processed at 750ºC and tested in monolithic configuration. Thus, the B/T texture obtained after processing at 1173 K (900 ºC) provides more isotropic mechanical properties to this multilayer laminate.

In summary, additional improvements in mechanical properties of Ti-6Al-4V multilayer materials are possible if the contribution of texture is taken into account. This is possible through the control of material phases during processing by changing conditions such as processing temperature. This opens new possibilities in this research area.

5. Conclusions

This research work has focused principally on the influence of microstructure and texture on the mechanical behavior of two Ti-6Al-4V multilayer materials processed by diffusion bonding at two temperatures (1023 and 1173 K (750 and 900 ºC)). The main conclusions are summarized as follows:

1. Microstructure, texture and mechanical properties at room temperature of the two processed laminates are influenced by the proportion of α/β phase in the microstructure during diffusion bonding processing.

2. The lowest processing temperature of 1023 K (750 ºC) maintains the as-received hot-rolled sheet texture, which is predominantly transversal in the longitudinal plane,

providing anisotropic mechanical behavior to the multilayer laminate. Accordingly, this laminate presents higher shear modulus (stiffness) and maximum shear strength when tested in the monolithic configuration due to the limited number of prismatic slip systems available during the shear test in this orientation.

3. The higher β phase proportion during diffusion bonding process at the highest temperature of 1173 K (900 ºC) leads to larger α grain size at room temperature, and a B/T texture of the α phase after partial $\alpha \rightarrow \beta \rightarrow \alpha$ transformations, which provides more isotropic properties to the multilayer material with respect to the laminate processed at 1023 K (750ºC). Therefore, the multilayer material processed at 1173 K (900 ºC) presents similar shear modulus and τ_{max} in both tested orientations (monolithic and interfacial), due to the presence of α grains favorably orientated for prismatic slip in both orientations.

4. The mechanical behavior of the Ti-6Al-4V multilayer materials can be tailored and optimized through control of microstructure and crystallographic texture changes occurring during thermomechanical processing.

Acknowledgements

Financial support from MICINN (Projects MAT2009-14452 and MAT2012-38962) is gratefully acknowledged. The authors thank Professor V. Amigó, M. J. Planes and A. Nuez from the electronic microscopy service at the Polytechnic University of Valencia, Spain, for experimental assistance with the EBSD technique.

References

1. H-S. Lee, J-H. Yoon, C.H. Park, Y.G. Ko, D.H. Shin and C.S. Lee: *J. Mater. Process. Technol.,* 2007, vol. 187-188, pp. 526-29.

2. J. Schneider, L. Dong, J.Y. Howe, and H.M. Meyer: *Metall. Mater. Trans A*, 2011, vol. 45, pp. 3527-33.

3. C.M. Cepeda-Jiménez, M. Pozuelo, J.M. García-Infanta, O.A. Ruano and F. Carreño: *Metall. Mater. Trans. A*, 2009, vol. 40, pp. 69-79.

4. A.A. Ganeeva, A.A. Kruglov and R.Ya. Lutfullin: *Rev. Adv. Mater. Sci.,* 2010, vol. 25, pp. 136-41.

5. J. Zhang and J.J. Lewandowski: *J. Mater. Sci.,* 1994, vol. 29, pp. 4022-26.

6. S. Nambu, M. Michiuchi, J. Inoue and T. Koseki: *Compos. Sci. Technol.,* 2009, vol. 69, pp. 1936-41.

7. C.M. Cepeda-Jiménez, P. Hidalgo, M. Pozuelo, O.A. Ruano and F. Carreño: *Mater. Sci. Eng. A,* 2010, vol. 527, pp. 2579-87.

8. A.G. Evans and J.W. Hutchinson: *Acta Metall. Mater*., 1995, vol. 43, 2507-30.

9. C.M. Cepeda-Jiménez, F. Carreño, O.A. Ruano, A.A. Sarkeeva, A.A. Kruglov and R.Ya. Lutfullin: *Mater. Sci. Eng. A,* 2013, vol. 563, pp. 28-35.

10. B.K. Kad, S.E. Schoenfeld and M.S. Burkins: *Mater. Sci. Eng. A*, 2002, vol. 322, pp. 241-51.

11. T. Vilaro, C. Colin, and J.D. Bartout: *Metall. Mater. Trans. A*, 2011, vol. 42, pp. 3190-99.

12. W.G. Burgers: *Physica*, 1934, vol. 1, pp. 561-86.

13. H.-R. Wenk, I. Lonardelli and D. Willians: *Acta Mater*., 2004, vol. 52, pp. 1899-907.

14. D. Bhattacharyya, G.B. Viswanathan, S.C. Vogel, D.J. Williams, V. Venkatesh and H.L. Fraser: *Scripta Mater*., 2006, vol. 54, pp. 231-36.

15. I. Lonardelli, N. Gey, H.-R. Wenk, M. Humbert, S.C. Vogel and L. Lutterotti: *Acta Mater*., 2007, vol. 55, pp. 5718-27.

16. G.A. Sargent, K.T. Kinsel, A.L. Pilchak, A.A. Salem, and S.L. Semiatin: *Metall. Mater. Trans. A*, 2012, vol. 43, pp. 3570-85.

17. G.E. Dieter: Mechanical Metallurgy, SI Metric, UK, 1988, pp.12-15.

18. S. Malinov, W. Sha, Z. Guo, C.C. Tang and A.E. Long: *Mater. Charact*., 2002, vol. 48, pp. 279-95.

19. R. Pederson, O. Babushkin, F. Skystedt and R. Warren: *Mater. Sci. Technol*., 2003, vol. 10, pp. 1533-38.

20. Titanium, G. Lutjering and J.C.Williams (eds), Springer-Verlag Berlin Heidelberg, 2nd edition, 2003.

21. J. Romero, M. Preuss and J. Quita da Fonseca: *Scripta Mater*., 2009, vol. 61, pp. 399-402.

22. Titanium and Titanium Alloys. C. Leyens and M. Peters (eds), Wiley-VCH, Weinheim, Germany, 2003, pp.8.

23. M.L. Meier, D.R. Lesuer and A.K. Mukherjee: *Mater. Sci. Eng. A*, 1991, vol. 136, pp. 71-8.

24. M. Karadge, M. Preuss, C. Lovell, P.J. Withers and S. Bray: *Mater. Sci. Eng. A*, 2007, vol. 459, pp. 182-92.

25. A.A. Salem, M.G. Glavicic and S.L. Semiatin: *Mater. Sci. Eng. A*, 2008, vol. 496, pp. 169-76.

26. N. Gey, M. Humbert and H. Moustahfid: *Scripta Mater*., 2000, vol. 42, pp. 525-30.

27. O.A. Kaibyshev, R.Ya. Lutfullin and V.K. Berdin: *Acta Metall. Mater*., 1994, vol. 42, pp. 2609-15.

28. W.J. Evans, J.P. Jones and M.T. Whittaker: *Int. J. Fatigue*, 2005, vol. 27, pp. 1244-50.

29. J. Gong and A.J. Wilkinson: *Acta Mater*., 2009, vol. 57, pp. 5693-705.

30. I. Bantounas, D. Dye and T.C. Lindley: *Acta Mater.*, 2010, vol. 58, pp. 3908-18.

Figure Captions

Figure 1. Schemes of: (a) the reference system considered in this work for multilayer composites; (b) tool employed for shear tests; and (c) different sample orientations for testing multilayer materials. SLD in the schemes is referred to shear load direction.

Figure 2. SEM micrographs showing a) the microstructure of the as-received Ti-6Al-4V alloy, and b) and c) the microstructure close to interfaces of Ti-6Al-4V multilayer laminates: b) processed at 1173 K (900 ºC), and c) processed at 1023 K (750 ºC). d) Schematic phase diagram in the $\alpha+\beta$ region of interest for multilayer laminates processing.

Figure 3. Pole figures for basal (0001) and prismatic (10-10) planes of the Ti-6Al-4V multilayer laminates in the LT section: a) Multilayer laminate processed at 1173 K (900 ºC), and b) processed at 1023 K (750 ºC). Schemes representing the main texture components in different planes (LT and L) are also included. c) Slip planes and slip directions in the *hcp* crystal structure of α-Ti.

Figure 4. Stress-strain curves from shear tests conducted on: a) monolithic and interfacial configurations; b) and various interfaces of the processed laminates.

Figure 5. EBSD inverse pole maps of different planes depicted in Fig. 1a for the Ti-6Al-4V multilayer laminate processed at 1023 K (750 ºC) close to the interface. a) LT plane, b) L plane and c) T plane. The EBSD maps have been color coded according to the inverse pole figure (IPF) shown in the inset, representing the crystallographic orientations parallel to the normal direction to each analyzed plane. Inverse pole figures showing the microtexture corresponding to the upper and bottom side of the interface in the LT plane are also included.

Figure 6. Schemes showing different orientations of the processed sample during shear tests. Additionally, the relative orientation of the hexagonal unit cell in different planes with respect to the shear load direction (SLD), and inverse pole figures that corroborate such crystallographic orientations are also included. a) Ti-6Al-4V multilayer laminate processed at 1023 K (750 ºC), and b) processed at 1173 K (900 ºC). 1. LT plane where macrotexture was characterized by XRD. 2. Interfacial plane (which coincides with the L plane). 3. Orientation considered to test the Ti-6Al-4V alloy in monolithic configuration, which coincides with the T plane.

Table 1. Mechanical properties of the monolithic Ti-6Al-4V alloy and interfaces in the Ti-6Al-4V multilayer laminates from shear tests (τ_{max}= maximum shear strength; $\gamma_{shear\ max.}$= maximum shear strain).

Material and shear testing orientation	**τ_{max} (MPa)**	**$\gamma_{shear\ max.}$**
Monolithic configuration:		
Processed at 1173 K (900 ºC)	481 ± 48	2.61 ± 0.52
Processed at 1023 K (750 ºC)	547 ± 8	2.07 ± 0.04
Interfacial configuration:		
Processed at 1173 K (900 ºC)	502 ± 13	1.34 ± 0.06
Processed at 1023 K (750 ºC)	455 ± 29	0.83 ± 0.05

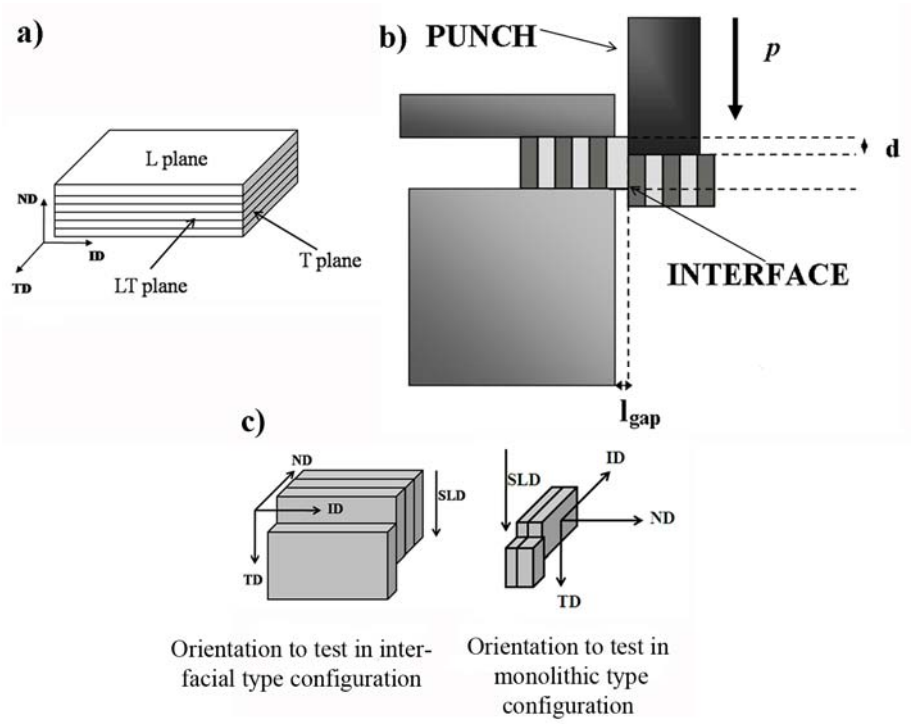

Figure 1. Schemes of: (a) the reference system considered in this work for multilayer composites; (b) tool employed for shear tests; and (c) different sample orientations for testing multilayer materials. SLD in the schemes is referred to shear load direction.

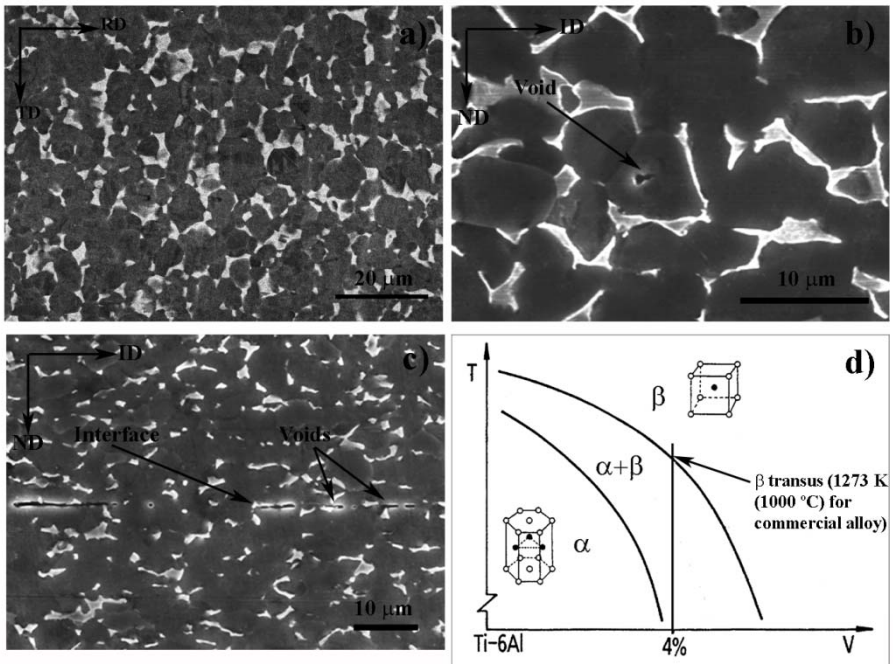

Figure 2. SEM micrographs showing a) the microstructure of the as-received Ti-6Al-4V alloy, and b) and c) the microstructure close to interfaces of Ti-6Al-4V multilayer laminates: b) processed at 1173 K (900 ºC), and c) processed at 1023 K (750 ºC). d) Schematic phase diagram in the α+β region of interest for multilayer laminates processing.

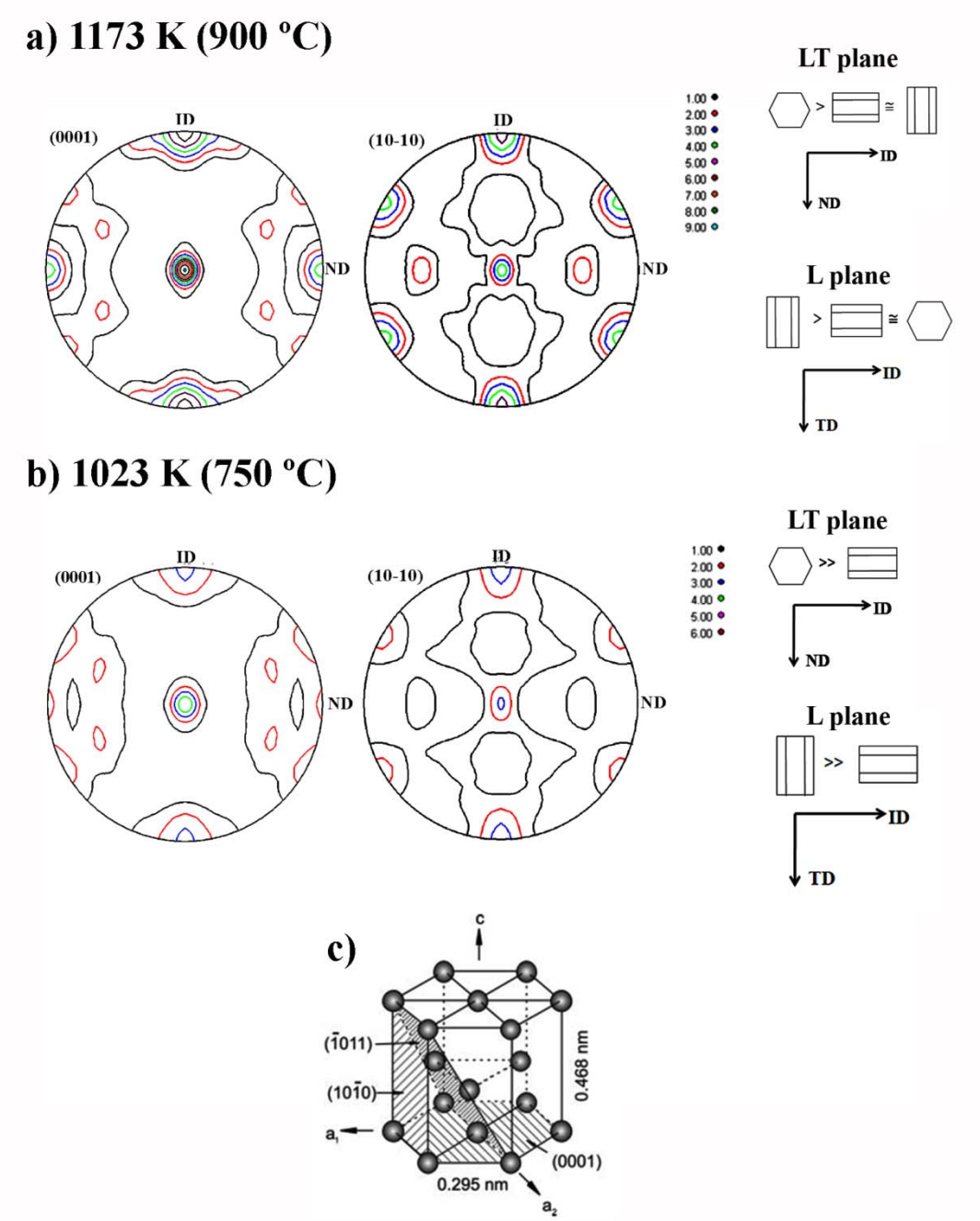

Figure 3. Pole figures for basal (0001) and prismatic (10-10) planes of the Ti-6Al-4V multilayer laminates in the LT section: a) Multilayer laminate processed at 1173 K (900 ºC), and b) processed at 1023 K (750 ºC). Schemes representing the main texture components in different planes (LT and L) are also included. c) Slip planes and slip directions in the *hcp* crystal structure of α-Ti.

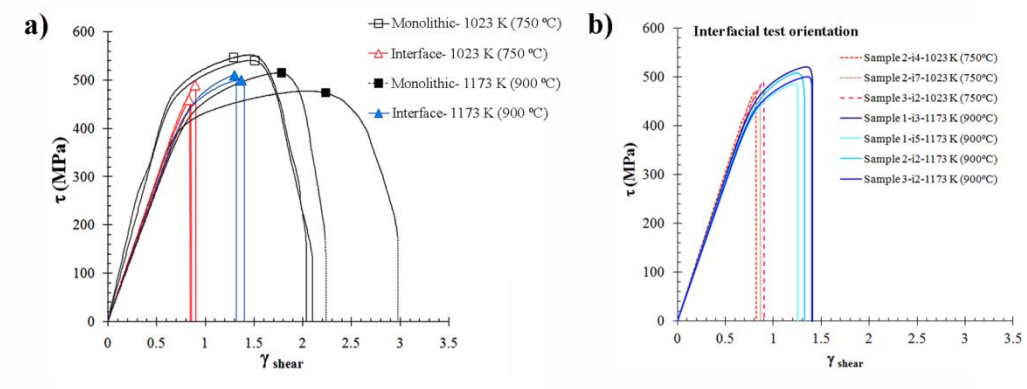

Figure 4. Stress-strain curves from shear tests conducted on: a) monolithic and interfacial configurations; b) and various interfaces of the processed laminates.

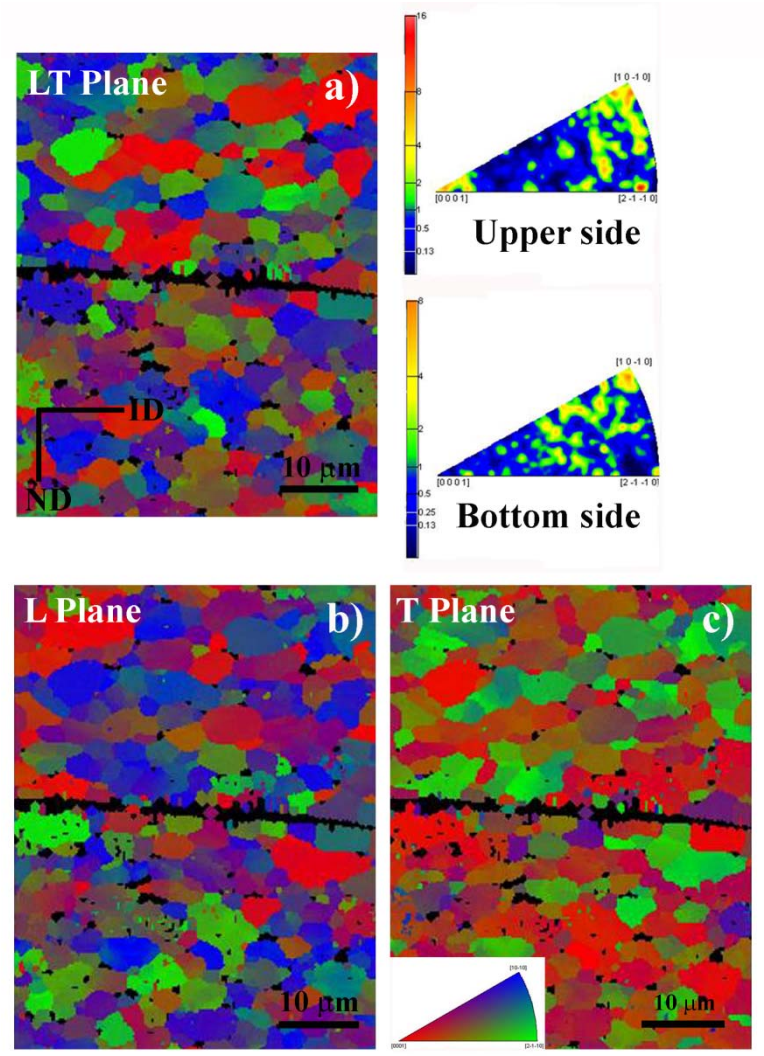

Figure 5. EBSD inverse pole maps of different planes depicted in Fig. 1a for the Ti-6Al-4V multilayer laminate processed at 1023 K (750 ºC) close to the interface. a) LT plane, b) L plane and c) T plane. The EBSD maps have been color coded according to the inverse pole figure (IPF) shown in the inset, representing the crystallographic orientations parallel to the normal direction to each analyzed plane. Inverse pole figures showing the microtexture corresponding to the upper and bottom side of the interface in the LT plane are also included.

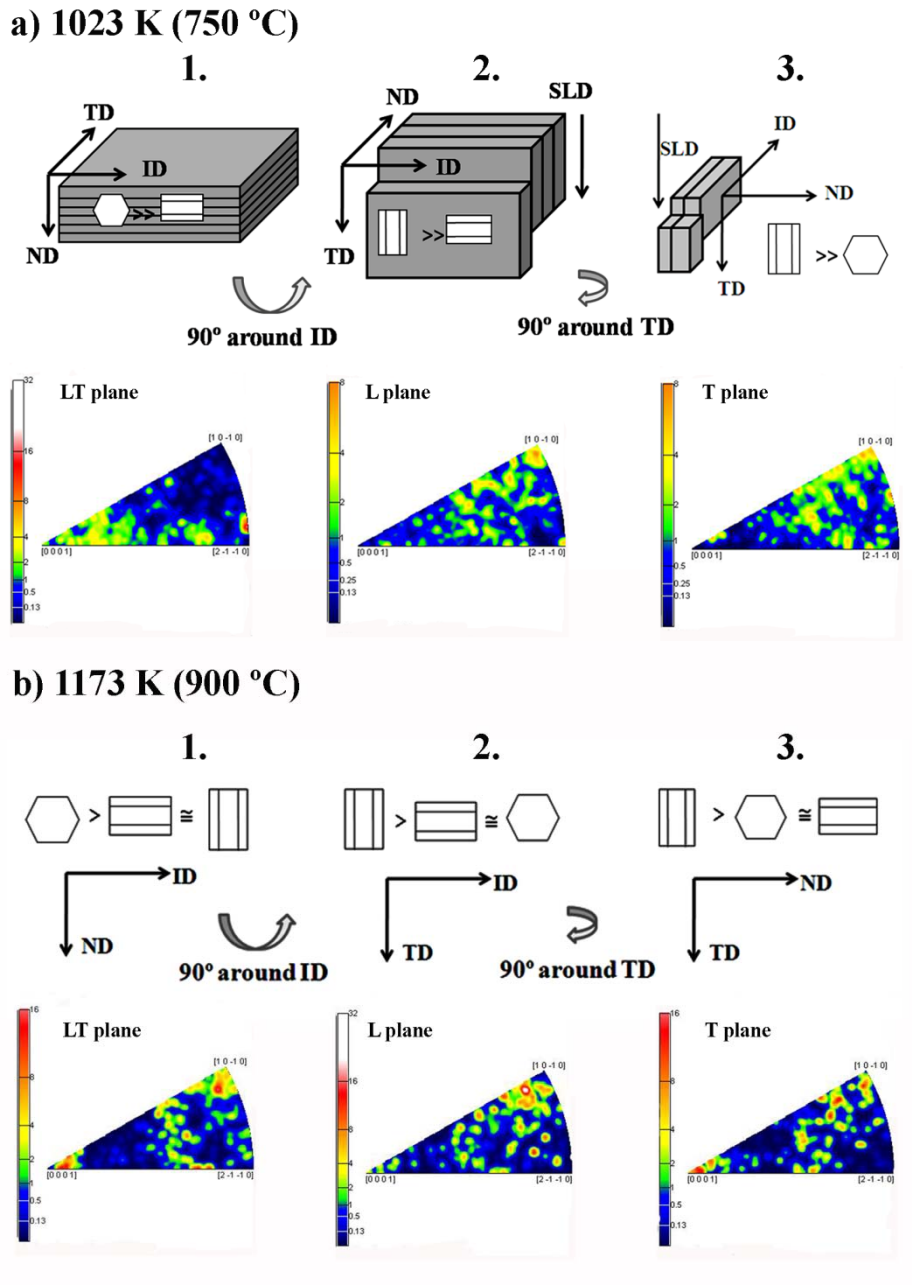

Figure 6. Schemes showing different orientations of the processed sample during shear tests. Additionally, the relative orientation of the hexagonal unit cell in different planes with respect to the shear load direction (SLD), and inverse pole figures that corroborate such crystallographic orientations are also included. a) Ti-6Al-4V multilayer laminate processed at 1023 K (750 ºC), and b) processed at 1173 K (900 ºC). 1. LT plane where macrotexture was characterized by XRD. 2. Interfacial plane (which coincides with the L plane). 3. Orientation considered to test the Ti-6Al-4V alloy in monolithic configuration, which coincides with the T plane.